View metadata, citation and similar papers at core.ac.uk

brought to you by CORE

provided by Loughborough University Institutional Repository

Cite this: DOI: 10.1039/c0xx00000x

www.rsc.org/xxxxxx

ARTICLE TYPE

Synthesis and photophysical properties of novel butterfly-shaped blue emitters based on pyrene

Xing Feng,[a] Jian-Yong Hu,*[a,b] Hirotsugu Tomiyasu,[a] Nobuyuki Seto,[a] Carl Redshaw,[c] Mark R. J. Elsegood[d] and Takehiko Yamato*[a]

Received (in XXX, XXX) Xth XXXXXXXXX 20XX, Accepted Xth XXXXXXXXX 20XX

DOI: 10.1039/b000000x

Using 1,3,5,9-tetrabromo-7-*tert*-butylpyrene as the bromide precursor, a series of novel butterfly-shaped 1,3,5,9-tetraaryl substituted pyrene derivatives were synthesized by the Suzuki-Miyaura cross-coupling reaction. Their thermal, photophysical, electrochemical and related properties were systematically investigated. All compounds were found to exhibit high thermal stabilities with decomposition temperatures (T_g) of up to 300 ºC. All compounds show highly blue fluorescence emissions in the spectral region of 412–469 nm in solutions (Φ_f: 0.45–0.92) and 410–470 nm in the solid-state (Φ_f: 0.48–0.75). In particular, the compounds **4e, 4f** and **5** show much greater red shifts because of the presence of the larger π-conjugated acceptor groups, which were verified by theoretical calculations. It is noteworthy that these butterfly-shaped pyrenes **4** possess low-lying HOMO levels ranging from –4.76 to –5.93 eV, which make them promising candidates in OLED applications.

Introduction

The design and synthesis of efficient organic semiconductors based on polycyclic aromatic hydrocarbons (PAHs) has attracted considerable interest, owing to their potential applications in optoelectronic devices,[1] such as organic light-emitting diodes (OLEDs), organic photovoltaics (OPVs), organic field-effect transistors (OFETs), etc. In the past two decades, significant efforts have been devoted to explore novel electroluminescent (EL) materials with specific optoelectronic properties.[1,2] To realize full-color OLED displays, the development of efficient and pure red, green and blue emitters is a significant milestone. However, only the red and green materials have been implemented in devices capable of sufficient efficiencies and lifetimes for commercial value,[3] whilst the availability of blue emitters with satisfactory multifunctional properties for high-performance OLEDs still remains a challenge.

Pyrenes[4] as classical members of the PAHs have attracted great interests from the scientific community, not only because of their planar structure, but also their excellent fluorescence properties, which has led to their wide utilization as fluorescence probes. Recently, a number of synthetic methods for the synthesis of novel PAHs based on pyrene have been reported,[5] and their potential uses as chemosensors were exploited.[6]

However, the flat structure of pyrene has restricted its use for developing EL materials for OLED applications, primarily because of the tendency towards π-stacking and excimer formations, which would quench the emission intensity with low fluorescence quantum efficiency. One strategy to suppress the passive π-π stacking interactions in condensed medias is to introduce appropriate substituents into the pyrene core. The methods tend to attach substituents at the 1-, 3-, 6- and 8-positions of the pyrene so as to affect both the overall photophysical properties and the geometrical structures. For example, 1,3,6,8-tetraphenylpyrene (TPPy) exhibited a pure blue fluorescence with a high quantum yield (Φ_f = 0.90 in cyclohexane).[7] Bulky aryl groups have been located at the 1,3,6,8-positions for the preparation of tetraaryl-functionalized pyrenes which showed high efficiencies with deep-blue emission, low turn-on voltages and high brightness in OLED devices.[8] Sotoyam and co-workers have investigated different phenyl moieties 1,3,6,8-tetrasubstituted pyrene and how they affect the fluorescent properties by molecular orbitals (MOs) methods.[9] The *tert*-Butyl groups located at the 2- or the 2- and 7-positions of the pyrene core play an important role in inhibiting the undesirable π-stacking interactions in the solid-state. Thus, the cruciform-, hand-, and Y-shaped pyrene derivatives were reported and can be potentially used as blue emitters in OLEDs.[10]

Previously, a novel bromide precursor 1,3,5,9-tetrabromo-7-*tert*-butylpyrene was prepared from 2-*tert*-butylpyrene and Br_2 in CH_2Cl_2 in the presence of iron powder (6 equiv.) at room temperature.[11] Based on this key intermadiate, herein, we access a series of butterfly-shaped compounds of 1,3,5,9-tetraarylpyrenes with deep-blue fluorescence properties. Several 4-substituted phenyl groups were successfully introduced into the pyrene core at the 1,3,5,9-positions. Not only does this category of materials have great potential in organic materials, such as blue emitters for OLED applications, but will also be useful to understand the structure-property relationships of the current butterfly-shaped 1,3,5,9-tetraarylpyrenes relative to the other arylpyrenes.

Results and discussion

Synthesis

The synthetic route to the butterfly-shaped pyrene derivatives **4a–f** are illustrated in Scheme 1. By using the 1,3,5,9-tetrabromo-7-*tert*-butylpyrene (**2**)[11] as the key intermediate, the compounds of type **4** were synthesized by the Suzuki-Miyaura cross-coupling reaction with the corresponding arylboronic acids (**3**) in 48–72% yields. To investigate the effect of a terminal moiety on the structure-property relationships in these butterfly-shaped pyrenes systems, the reaction of **4f** with 17.0 equiv. of hydroxylamine hydrochloride in ethanol solution afforded the corresponding oxime **5** in 76% yield according to the literature approach.[12] Furthermore, in order to investigate the effect of the *tert*-butyl group of the pyrene on photophysical properties, **6** was synthesized from **4a**, in which the bulky steric *tert*-butyl group has been removed by Nafion-H catalyzing.[13] The chemical structures of all synthesized compounds were confirmed by their $^{1}H/^{13}C$ NMR spectra, FT-IR spectroscopy, mass spectrometry, as well as elemental analysis.

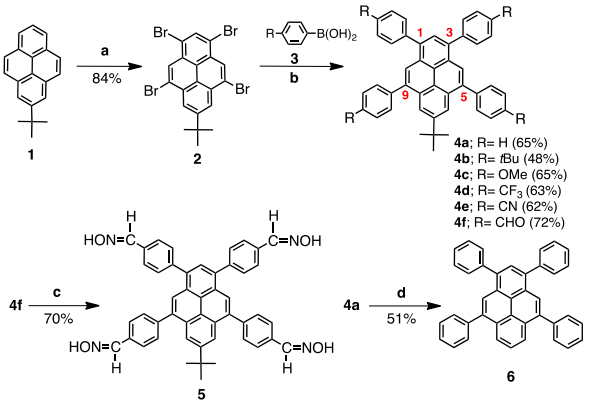

Scheme 1 Synthetic route to the compounds **4**, **5** and **6**. Reagents and conditions: (a) iron powder, Br_2, CH_2Cl_2, room temp., 4 h, 84%. (b) $Pd(PPh_3)_4$, toluene, K_2CO_3, 90 °C, 24 h. (c) $NH_2OH{\cdot}HCl$, ethanol, NaOH, reflux, 12 h. (d) Nafion-H, *o*-xylene, 160 °C, 24 h.

Thermal properties

Thermal stability is an important physical parameter to evaluate EL materials for OLED applications. We investigated the thermal stability of these butterfly-shaped pyrene derivatives **4** and **5** by thermogravimetric analysis (TGA) and differential scanning calorimetry (DSC) under a nitrogen atmosphere at a heating rate of 10 °C min^{-1}. The TGA data revealed that the butterfly-shaped compounds **4** showed high thermal stabilities in the range of 250–450 °C, with a 5% weight loss. (Fig. 1), and the following stability order CN > OMe > *t*-Bu > H > CHO > CF_3 > **5**. From the TGA data, the amount of carbonized residue (char yield) of **4c**, **4e**, **4f** and **5** in a nitrogen atmosphere was higher (20% for **4c**, **4f**, 37% for **4e** and 64% for **5**) than **4a**, **4b** and **4d** with almost complete loss, which means that **4c, 4e, 4f** and **5** possess more aromatic components than **4a, 4b** and **4d**.[14] Ascribe from the substituent group [What does this mean? Please re-write.] at *para*-position of the phenyl would affect the thermal property. No glass transition temperature (T_g) was observed for any of the compounds.

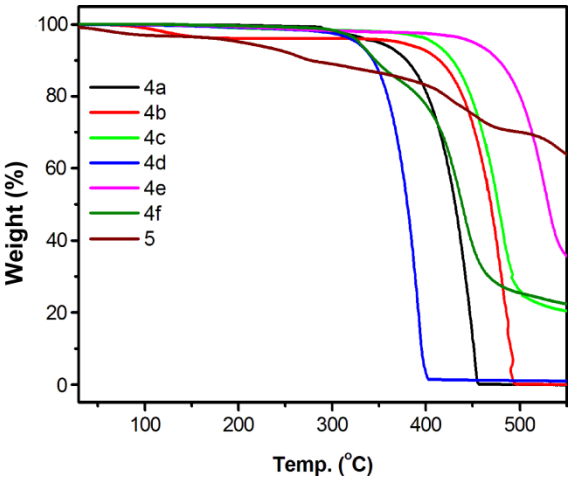

Fig. 1 TGA curves of compounds **4** and **5**.

Photophysical properties

We measured the UV-vis absorption and fluorescence (FL) spectra of compounds **4**–**6** in both dichloromethane solutions (~10^{-5} M) and thin films. The key data are summarized in Table 1.

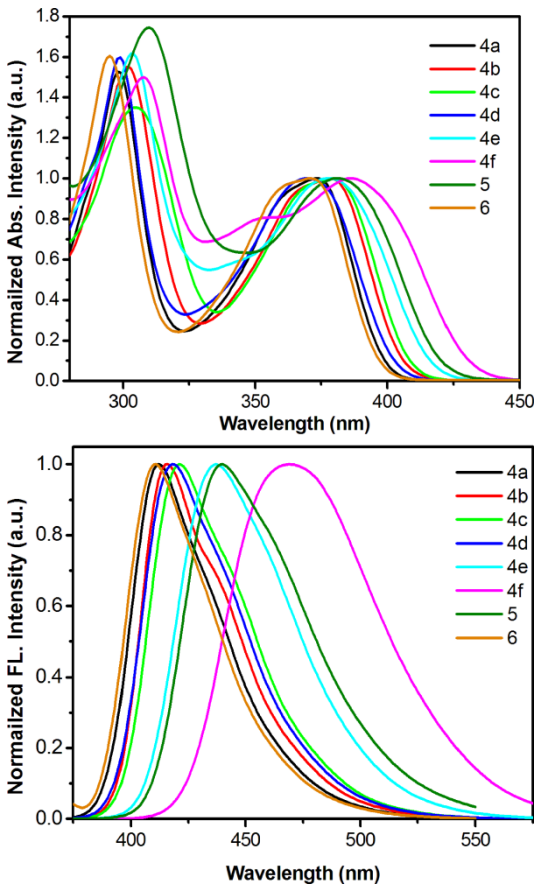

Fig. 2 (a) Normalized UV-vis absorption and (b) fluorescence emission spectra of compounds **4** and **5** recorded in dichloromethane solutions at ~10^{-5}–10^{-6} M at 25 °C.

Table 1 The photophysical and electrochemical properties of compounds **4**, **5** and **6**.

Compound	λ_{max} abs (nm)		λ_{max} PL (nm)		Φ_f^c	Stokes shift (cm^{-1})	τ (ns)	T_m^d/ T_d^e (°C)
	solns[a]	/ films[b]	solns[a]	/ films[b]	solns / thin films	solns[a] / films[b]		
4a	373	380	412	410	0.92 / 0.75	39 / 30	4.57	335/350
4b	378	379	416	435	0.45 / nd	38 / 56	5.18	332/407
4c	379	369	421	443	0.90 / 0.72	42 / 74	5.82	330/410
4d	370	358	418	466	0.91 / nd	48 / 108	12.2	258/328
4e	378	387	437	460	0.89 / nd	59 / 73	7.51	378/450
4f	386	400	469	471	0.56 / 0.48	83 / 71	4.04	302/329
5	381	nd	440	nd	0.63 / nd	59 / nd	4.53	214/250
6	371	nd	411	nd	0.26 / nd	40 / nd	5.10	244/nd

[a] Maximum absorption wavelength measured in dichloromethane at room temperature. [b] Measured as thin neat films. [c] Measured in dichloromethane and as neat thin films, respectively. [d] Melting temperature (T_m) obtained from differential scanning calorimetry (DSC) measurements. [e] Decomposition temperature (T_d) obtained from thermogravimetric analysis (TGA). nd: not determined.

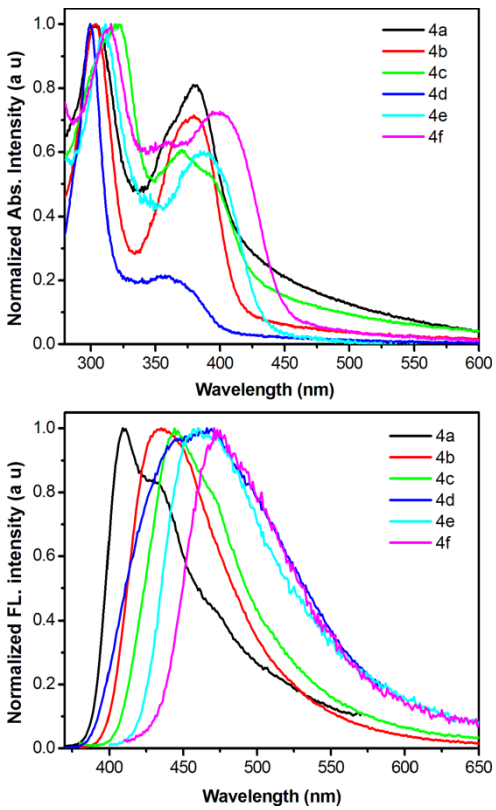

Fig. 3 (a) Normalized UV-vis absorption and (b) emission spectra of **4a–f** as thin neat films.

Fig. 2 illustrates the normalized absorption and FL spectra of of **4**, **5** and **6** in dilute dichloromethane solutions. The absorption spectra of these butterfly-shaped pyrene derivatives **4** and **6** exhibited well-resolved profiles in the range of 280–480 nm. The short wavelength absorption peak located at 277–279 nm and the long wavelength maximum (λ_{max}) occur at 370–381 nm, assigned to the π-π* and the n-π* transitions (Fig. 2a), respectively. Noticeably, **4f** and **5** showed slightly red shifts of ~10 nm compared to the other compounds due to the effective increase in conjugation length. It is noteworthy that the compound **6** exhibited a blue shift (8 nm) after the removal of the *tert*-butyl group from the 2-position of the pyrene core compared to **4c**, arising from the improved energies of both $S_1 \leftarrow S_0$ excitations and $S_2 \leftarrow S_0$ excitations.[15]

Upon excitation at the absorption maximum in CH_2Cl_2, all compounds exhibited deep-blue to sky-blue FL with sharp emission maximum peaks at 412 nm for **4a**, 416 nm for **4b**, 421 nm for **4c**, 418 nm for **4d**, 437 nm for **4e**, 440 nm for **5** and 411nm for **6** (Fig. 2b). In the case of **4f**, which showed a maximum peak at 469 nm, there was a larger Stokes shift of 83 nm relative to the other butterfly-shaped compounds, suggesting that its electronic structure in the ground state is significantly different from that in the excited state. It is noted that **4e** and **5** showed almost the same emission peaks, suggesting that the –C≡N and –C=N-OH groups make similar electronic contibutions. This result implies that changing the terminal group at the *para*-position of the phenyl moiety can affect the electron transition absorption, which also agrees with our previous report.[10a] Furthermore, a substituent effect involving $S_1 \leftarrow S_0$ was also observed in the emission spectra, and without the *tert*-butyl group in compound **6**, the emission maximum displayed a lower red shift of ~10 nm compared to the corresponding compound **4c**.

We also investigated the photophysical properties of **4** in the solid-state. The UV-vis absorption and photoluminescence (PL) spectra data are also listed in Table 1. As shown in Fig. 3, the absorption spectra of these butterfly-shaped pyrenes **4**, possessing similar frameworks (pyrene-based core), exhibited a similar absorption band with a slight red shift (~14 nm) to those in dilute solutions. Compared with the FL in solutions, the PL spectra of **4a–f** and **5** in thin films exhibited highly blue emissions with a maximum peak in the range of 410–471 nm, without extra excimer emissions, while compounds **4b–e** displayed a red-shift (~48 nm), ascribed to the *tert*-butyl group located at the 7-position and the tetraaryl moieties at the 1,3,5,9-positions which can prevent π-aggregations via the intra/intermolecular interactions in the solid-state. The single-crystal packing revealed that no π-π stacking was observed,[11] however, the aggregations cannot be sufficiently suppressed[16] due to the small blocking group of the arylphenyl located at the 1,3,5,9-positions. Thus, larger red-shifts occurred in **4c** and **4d**. Fig. 2b and 3b revealed that these butterfly-shaped compounds **4** and **5** emit very bright and sharp blue fluorescence in both solution and the solid-state. The newly developed butterfly-shaped pyrenes **4a–e** and **5** have very high quantum yields (Φ_f) in the range of 0.89–0.92 in solutions and 0.72–0.78 in the solid-state. Due to the presence of

Table 2 Optical and electrochemical properties of compounds **4**, **5** and **6**.

	λ_{edge} [a]/nm	$E_{1/2}$ [b]	E_{onset} [b]	$E_{gap(opt)}$ [c]/eV	$E_{HOMO(CV)}$ [d]/eV	$E_{HOMO(cal)}$ [e]/eV	$E_{gap(calcd)}$ [e]
4a	399	1.42	1.35	3.11	–5.56	–5.01	3.43
4b	405	1.35	1.27	3.06	–5.51	–4.90	3.40
4c	411	1.28	1.20	3.01	–5.44	–4.76	3.40
4d	403	1.66	1.58	3.08	–5.82	–5.61	3.40
4e	418	1.71	1.63	2.97	–5.87	–5.93	3.32
4f	431	1.67	1.58	2.88	–5.82	–5.66	3.21
5	419	1.41	1.29	2.96	–5.56	–5.25	3.24
6	397	–	–	3.12	–	–5.06	3.43

[a] Measured in CH_2Cl_2. [b] CV measured in 0.1 M *n*-Bu_4NPF_6/CH_2Cl_2 with a scan rate of 100 mV s^{-1}; [c] Calculated from λ_{edge}. [d] values calculated using the ferrocene HOMO level: Calculated from the empirical formulae HOMO = -(4.8 + $E_{ox}^{1/2}$ -$E_{ox\ (Fc)}^{1/2}$), [e] DFT/B3LYP/6-31G* using Gaussian 03.

the –CHO in **4f** that has efficient intramolecular conjugation and increased π–π intermolecular interactions that would quench the FL with quantum yields of 0.56 in solution and 0.48 in the solid-state. However, **6** exhibited a lower quantum yield of 0.26 compared with the TPPy (Φ_f = 0.90),[7] which is probably due to the strong intermolecular interactions without the bulky steric *tert*-butyl group. Fluorescence lifetimes of **4**–**6** were determined in dichloromethane solution at 10^{-5} M with τ = 4.04–12.2 ns.

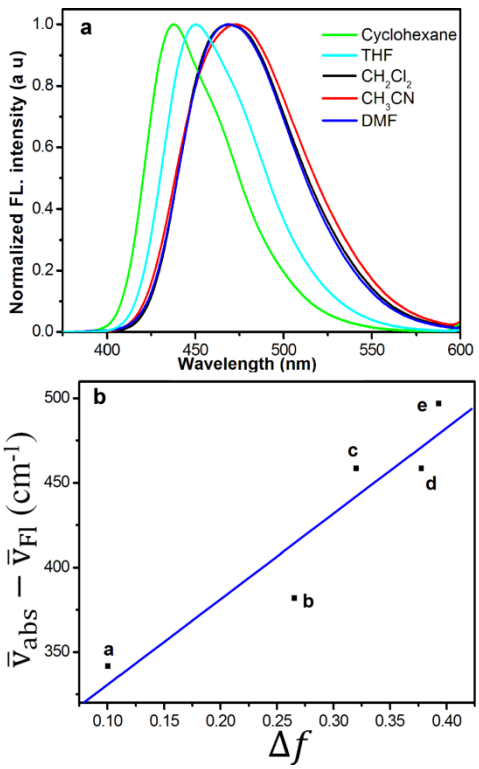

Fig. 4 (a) Emission spectra of **4f** in cyclohexane, THF, CH_2Cl_2, CH_3CN and DMF at 25 °C. (b) Lippert-Mataga plots for compound **4c** (CHO): (a) cyclohexane, (b) CH_2Cl_2, (c) THF, (d) DMF, (d) CH_3CN.

Concentration-dependent UV-vis absorption and FL spectra studies in CH_2Cl_2 confirmed that these compounds did not change with concentration in solution, even on increasing the concentrations from 10^{-6} M to 10^{-3} M (See Supporting Information). On the other hand, we examined the solvatochromism of **4** and **5** in various solvents, such as cyclohexane, tetrahydrofuran (THF), CH_2Cl_2, CH_3CN, and *N*,*N*-dimethylformamide (DMF) (Fig. 4a). In the compounds **4a**–**e** and **5**, the emission maxima were slightly shifted by ~5 nm depending on the solvent polarity. However, although the absorption spectrum of compound **4f** does not show any change, the solvent dependence in the emission spectra of **4f** is remarkable with large bathochromic shifts of ~36 nm on going from non-polar solvents (cyclohexane) to polar solvents (DMF). The linear relationship of Stokes shift ($\Delta\nu_{st}$) against the solvent parameter $\Delta_f(\varepsilon, n)$[17] was determined by the Lippert–Mataga plot (Fig. 4b), which evaluated the effect of solvent molecules for day molecules fluorescence by hydrogen bond [This does not make any sense – please re-write].[18] This solvatochromism can be attributed to the decrease in the energy of the singlet-excited states as a function of an increase in the polarity of the solvents.[19]

$$\Delta\nu = \frac{1}{4\pi\varepsilon_0 hca^3}\ \frac{2\Delta\mu^2}{hcR^3}\ \Delta f + \text{const} \qquad (1)$$

where $\triangle\nu = \nu_{abs}-\nu_{em}$ stands for Stokes shift, ν_{abs} is wavenumber of maximum absorption, ν_{em} is the wavenumber of maximum emission, $\Delta\mu = \mu_e - \mu_g$ is the difference in the dipole moment of solute molecule between excited (μ_e) and ground (μ_g) states, *h* is Planck's constant, R is is the radius of the solvent cavity in which the fluorophore resides (Onsager cavity radius), and Δf is the orientation polarizability given by (Eq. 2)

$$\Delta f = \frac{\varepsilon-1}{2\varepsilon+1} - \frac{n^2-1}{2n^2+1} \qquad (2)$$

where ε is the static dielectric constant and *n* the refractive index of the solvent.

Electrochemical properties

We investigated the electrochemical properties of these compounds by cyclic voltammetry (CV) recorded in CH_2Cl_2 solution using ferrocene (Fc/Fc^+) as the internal standard with a scan rate of 100 mVs^{-1} at room temperature. Fig. 5 displays the cyclic voltammograms (CVs) of **4** and **5**. All compounds exhibited quasi-reversible oxidations in CH_2Cl_2. Interestingly, the compounds **4b** and **4c**, with electron-donating groups, showed two reversible oxidation waves, while the compounds **4d–f** and **5**, with electron-withdrawing groups, have only one reversible oxidation each. These results differ from the Y-shaped compounds that we recently reported,[10c] Obviously, the substituent positions play a significant role in affecting the

Cite this: DOI: 10.1039/c0xx00000x

www.rsc.org/xxxxxx

ARTICLE TYPE

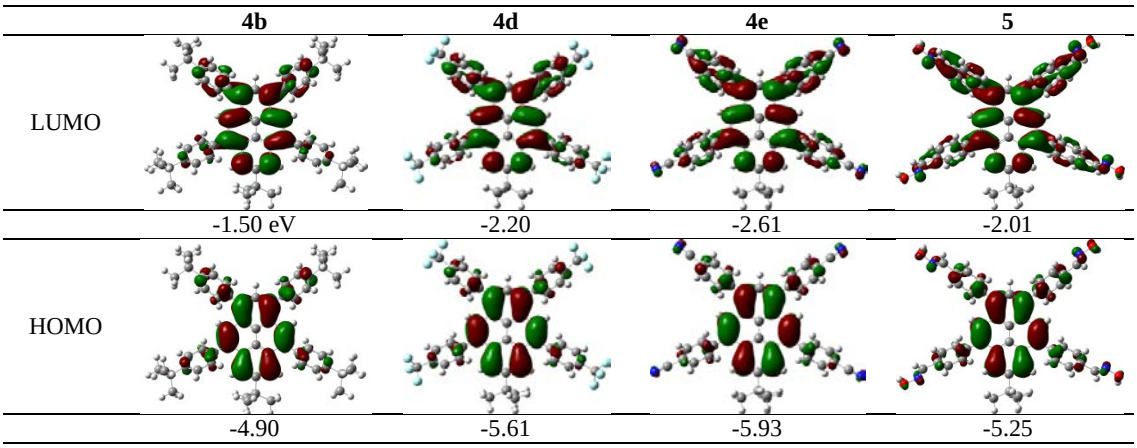

Fig. 6 Computed molecular orbital plots (B3LYP/6–31G*) of **4** and **5**.

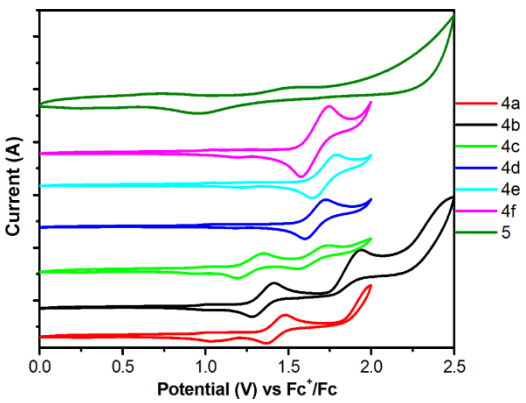

Fig. 5 Cyclic voltammograms recorded for compounds **4** and **5**.

electronic structure and reversible oxidation characteristics. They are also clearly affected by the donator/acceptor groups of the arylphenyl moieties at the 5,9- positions of the pyrene core in the current butterfly-shaped pyrenes.[15] Accordingly, the HOMO and LUMO energy levels were estimated from the CVs and the UV-vis absorption and the data are summarized in Table 2. The HOMO energy levels increased from –5.36 to –5.79 eV in the order: **4e** > **4d** > **4f** > **4a** > **4b** = **5** > **4c**, and their LUMO energy levels were in the range –2.36 to –2.96 eV. Based on the HOMO and LUMO energy levels, it can be proposed that these newly developed blue emitters **4** and **5** could be used as blue emitters in OLEDs.

To further understand the electronic properties of **4, 5** and **6**, DFT calculations (B3LYP/6–31G* basis set) were carried out using Gaussian 03 for the geometry optimization.[20] The optimized structures and orbital distributions of the HOMO and LUMO of these butterfly-shaped pyrenes are shown in both Fig. 6 and the supporting information. The dihedral angles between the arylphenyl and pyrene are in the range of 55–58°, which suggested that the different substituents equally contribute to the steric congestion in these system. The HOMO levels of **4**, **5** and **6** mainly involve contributions of π-orbitals from the pyrene core, while the substituent aryl groups have limited contributions to these molecules. Similarly, the LUMO levels are also spread across the entire pyrene frameworks; however, acceptor groups with π-conjugation enlarged range from –CF_3, –CN, –CHO and –C=N–OH, the LUMOs located on entire molecules [I don't understand this sentence – please re-write]. The HOMO-LUMO energy gaps were in the range of 3.21 eV to 3.43 eV in **4** and **5**. Therefore, these theoretical calculations provided clear evidence that the red shift of the absorption and emission bands observed in compounds **4** and **5** are consistent with the experimental results. Without the *tert*-butyl group in **6**, the energy gap resembles that of **4a**, but with a lower LUMO energy level.

Conclusion

In summary, in this study, a series of novel butterfly-shaped pyrene derivatives was successfully synthesized by the classical Suzuki-Miyaura cross-coupling reaction. The introduction of several arylphenyl substituents located at the 1,3,5,9-positions of the pyrene influenced the FL emissions in solution and in the solid-state. The structure-property relationships of the donor–acceptor interactions play a curial role in determining the thermal, UV-vis absorption, electrochemical behavior, etc. These pyrenes possess high solubility, high stability, highly blue emissions with quantum efficiency of up to 70%, and long fluorescence lifetimes in solution. These excellent qualities make them very promising for applications in OLED devices.

Experimental

General

All melting points (Yanagimoto MP-S_1) are uncorrected. ^{1}H NMR spectra (300 MHz) were recorded on a Nippon Denshi JEOL FT-300 NMR

spectrometer with $SiMe_4$ as an internal reference: *J*-values are given in Hz. IR spectra were measured for samples as KBr pellets in a Nippon Denshi JIR-AQ2OM spectrophotometer. UV-Vis spectra were measured using a Shimadzu UV-3150 UV-vis-NIR spectrophotometer. Fluorescence spectroscopic studies of compounds in solution were performed in various organic solvents in a semimicro fluorescence cell (Hellma®, 104F-QS, 10 × 4 mm, 1400 μL) with a Varian Cary Eclipse spectrophotometer, and Photoluminescence spectra of compounds in film were obtained using a FluroMax-2 (Jobin-Yvon-Spex) luminescence spectrometer. Fluorescence quantum yields were measured (Hamamatsu Photonics K. K, Quantaurus-QY A10094) using integrated sphere absolute PL quantum yield measurement method. The luminescence lifetimes of the bufferfly-shaped compounds were obtained with Hamamatsu Photonics OB920 by using nanoLED excitation sources at 373 (ligand) or the maximum λ_{em} of days {I don't understand what this means 'of days'.}. Thermogravimetric analysis (TGA) was carried out using a SEIKO EXSTAR 6000 TG/DTA 6200 unit under nitrogen atmosphere at a heating rate of 10 °C min^{-1}. Differential scanning calorimetery (DSC) was performed using a Perkin–Elmer Diamond DSC Pyris instrument under a nitrogen atmosphere at a heating rate of 10 °C min^{-1}. Mass Spectrometer at 75 eV using a direct-inlet system [Not a proper sentence]. Elemental analyses were performed with a Yanaco MT-5 analyser. Cyclic voltammetry measurements were conducted using an ALS/H CH Instruments Electrochemical Analyzer 660B with a standard three-electrode configuration. Typically, a three-electrode cell equipped with a Pt disk working electrode, a Pt wire counter electrode and an $Ag/AgNO_3$ (0.01 M in anhydrous acetonitrile) reference electrode was employed. The measurements were made in anhydrous dichloromethane (for oxidation) with 0.1 M *n*-tetrabutylammonium hexafluorophosphate as the supporting electrolyte under an argon atmosphere at a scan rate of 100 mV/s. The potential of the $Ag/AgNO_3$ reference electrode was internally calibrated by using the ferrocene/ferrocenium redox couple (Fc/Fc^+).

Materials: Unless otherwise stated, all other reagents used were purchased from commercial sources and used without further purification. The preparation of 2-*tert*-butylpyrene (**1**) was described previously.[21]

Synthesis of 2-*tert*-butylpyrene (1).[20] A mixture of pyrene (5 g (more s.f. needed), 24.2 mmol) and 2-chloro-2-methylpropane (2.62 g, 3.23 mL) was added in 40 mL of CH_2Cl_2 at 0 °C and stirred for 15 min. Powdered anhydrous $AlCl_3$ (3.62 g, 27.2 mmol) was slowly added to the stirred solution. The reaction mixture was continuously stirred for 3 h at room temperature and the reaction process was tracked by GC, and then poured into a large excess of ice/water. The reaction mixture was extracted with dichloromethane (2 × 50 mL). The combined organic extracts were washed by water and brine, dried with anhydrous $MgSO_4$ and evaporated. The residue was crystallized from hexane to afford pure 2-*tert*-butylpyrene **1** (4.56 g, 71.4%) as a gray powder. Recrystallization from hexane gave **1** as colorless prisms. M.p. 111.5–113.2 °C (lit.[20] M.p. 110–112 °C). The ^{1}H NMR spectrum completely agreed with the reported values. ^{1}H NMR (300 MHz, $CDCl_3$): δ = 1.59 (s, 9H, *t*Bu), 8.18 (d, *J* = 9.2 Hz, 2H, pyrene-*H*), 8.30 (s, 2H, pyrene-*H*), 8.37 (d, *J* = 9.2 Hz, 2H, pyrene-*H*) and 8.47 (s, 1H, pyrene-*H*) ppm.

Lewis acid-catalysed bromination of 2-*tert*-butylpyrene (1). A mixture of 2-*tert*-butylpyrene (0.512 g, 2 (more s.f. needed) mmol) and iron powder (0.56 g, 10 mmol) was added while stirring for 15 min in CH_2Cl_2 (10 mL) at room temperature. Then, a solution of Br_2 (0.63 mL, 12.1 mmol) in CH_2Cl_2 (15 mL) was slowly added dropwise with vigorous stirring. After this addition, the reaction mixture was continuously stirred for 4 h at room temperature. The mixture was quenched with $Na_2S_2O_3$ (10%) and extracted with dichloromethane (2 × 50 mL). The combined organic extracts were washed with water and brine and then evaporated. The crude product exhibits a gray color. The crude product was insoluble in general common organic solvents, such as benzene, hexane, methanol, etc. and only slightly dissolved in CH_2Cl_2 or $CHCl_3$. Thus, the residue was dissolved in hot $CHCl_3$ and filtered, then crystallizeation from $CHCl_3$ to gave pure 7-*tert*-butyl-1,3,5,9-tetrabromopyrene **2** (978 mg, 84%) as colourless prisms. M.p. 303.4–305.0 °C; IR: ν_{max} (KBr)/cm^{-1}: 2962, 2365, 1579, 1523, 1461, 1425, 1392, 1363, 1267, 1195, 1132, 1027, 1012, 941, 877, 809, 655 and 474; ^{1}H NMR (300 MHz, $CDCl_3$): δ = 1.65 (s, 9H, *t*Bu), 8.47 (s, 1H, pyrene-*H*$_2$), 8.71 (s, 2H, pyrene-*H*) and 8.79 (s, 2H, pyrene-*H*) ppm. Due to the poor solubility, it was not further identified by ^{13}C NMR spectroscopy. FABMS: *m/z*: 573.62 [M^+]. $C_{20}H_{14}Br_4$ (573.78): calcd C 41.85, H 2.46; found: C 42.05, H 2.53.

Synthesis of 1,3,5,9-tetraaryl-7-*tert*-butylpyrenes (4). The series of butterfly-shaped compound **4a–f** were synthesized from 1,3,5,9-tetrabromo-7-*tert*-butylpyrene **2** with the corresponding arylboronic acid **3** by a Suzuki-Miyaura cross-coupling reaction in high yield.

Synthesis 7-*tert*-butyl-1,3,5,9-tetraphenylpyrene (4a). 7-*tert*-Butyl-1,3,5,9-tetrabromopyrene **2** (200 mg, 0.35 mmoL), phenylboronic acid **3a** (245 mg, 2.11 mmol), $Pd(PPh_3)_4$ (70 mg, 0.06 {more s.f needed} mmol), and K_2CO_3 (0.5 {more s.f needed} g, 3.6 mmol) were mixed in a flask containing argon saturated toluene (10 mL) and ethanol (4 mL). The reaction mixture was stirred at 90 °C for 24 h. After it was cooled to room temperature, the reaction mixture was extracted with dichloromethane (3 × 50 mL), and the organic layer was washed with H_2O and brine, then dried with anhydrous $MgSO_4$ and evaporated. The crude product was purified by column chromatography using dichloromethane as eluent to afford a deep yellow solid. Recrystallization from a mixture of CH_2Cl_2–methanol (2:1) gave **4a** (128 mg, 65%) as colourless needles. M.p. 335 °C. IR: ν_{max} (KBr)/cm^{-1}: 3422.5, 2961.0, 2366.6, 1593.2, 1496.6, 1363.8, 1252.8, 1177.6, 1070.3, 894.7, 762.3, 701.3, 626.1 and 483.1. ^{1}H NMR (400 MHz, $CDCl_3$): δ = 1.36 (s, 9H, *t*Bu), 7.40−7.54 (m, 12H, Ar-*H*), 7.63−7.70 (m, 8H, Ar-*H*), 7.98 (s, 1H, pyrene-*H*), 8.16 (s, 2H, pyrene-*H*) and 8.29 (s, 2H, pyrene-*H*) ppm. ^{13}C NMR (100 MHz, $CDCl_3$): δ = 148.6, 141.4, 141.1, 139.8, 137.2, 130.6, 130.5, 130.1, 129.7, 128.4, 128.3, 127.4, 127.3, 127.2, 125.5, 124.5, 124.1, 121.4, 35.4 and 31.6 ppm. FABMS: *m/z*: 562.28 (M^+). $C_{44}H_{34}$ (562.74): calcd C 93.62, H 5.38; found: C 93.25., H 5.25.

7-*tert*-Butyl-1,3,5,9-tetrakis(4-*tert*-butylphenyl)pyrene (4b): Colourless prisms (CH_2Cl_2:methanol, 2:1) (132 mg, 48%). M.p. 332 °C. IR: ν_{max} (KBr)/cm^{-1}: 2964, 1596, 1510, 1460, 1396, 1363, 1270, 1109, 1023, 901, 833, 572 and 482. ^{1}H NMR (400 MHz, $CDCl_3$): δ = 1.39 (s, 9H, pyrene-tBu), 1.42 (s, 18H, phenyl-tBu), δ_H: 1.44 (s, 18H, pyrene-tBu), 7.54 (d, *J* = 8.4 Hz, 4H, Ar-*H*), 7.57 (d, *J* = 8.8 Hz, 4H, Ar-*H*), 7.62 (d, *J* = 7.6 Hz, 4H, Ar-*H*), 7.63 (d, *J* = 7.6 Hz, 4H, Ar-*H*), 7.98 (s, 1H, pyrene-*H*), 8.26 (s, 2H, pyrene-*H*) and 8.33 (s, 2H, pyrene-*H*) ppm. ^{13}C NMR (100 MHz, $CDCl_3$): δ = 150.2, 149.9, 148.3, 139.3, 138.5, 138.2, 137.0, 130.6, 130.3, 130.0, 129.9, 128.9, 127.2, 125.7, 125.3, 125.2, 124.4, 124.2, 121.2, 35.4, 34.7, 34.6, 31.7 and 31.4 ppm. FABMS: *m/z*: 786.58

[M^+]. $C_{60}H_{66}$ (786.52): C 91.55, H 8.45; found: C 91.25, H 8.55.

7-*tert*-Butyl-1,3,5,9-tetrakis(4-methoxyphenyl)pyrene (4c). Yellow prisms (CH_2Cl_2–methanol, 2:1) (154 mg, 65%). M.p. 330 °C. IR: ν_{max} (KBr)/cm^{-1}: 3437, 2957, 1610, 1507, 1457, 1285, 1246, 1174, 1106, 1038, 830, 583 and 540. ^{1}H NMR (400 MHz, $CDCl_3$): δ = 1.38 (s, 9H, *t*Bu), 3.90 (s, 6H, O*Me*), 3.92 (s, 6H, O*Me*), 7.06 (d, *J* = 8.8 Hz, 4H, Ar-*H*), 7.07 (d, *J* = 8.8 Hz, 4H, Ar-*H*), 7.56 (d, *J* = 8.6 Hz, 4H, Ar-*H*), 7.60 (d, *J* = 8.8 Hz, 4H, Ar-*H*), 7.92 (s, 1H, pyrene-*H*), 8.12 (s, 2H, pyrene-*H*) and 8.30 (s, 2H, pyrene-*H*) ppm; ^{13}C NMR (100 MHz, $CDCl_3$) δ = 159.0, 158.9, 148.5, 139.1, 136.7, 133.9, 133.7, 131.7, 131.2, 130.8, 129.7, 127.3, 125.6, 121.2, 113.9, 113.8, 55.4 and 31.7 ppm; FABMS: *m/z*: 682.19 [M^+]. $C_{48}H_{42}O_4$ (682.31): calcd C 84.43, H 6.20; found: C 84.01, H 5.93.

7-*tert*-Butyl-tetrakis-1,3,5,9-(4-trifluorophenyl)pyrene (4d). Colourless prisms (CH_2Cl_2–methanol, 2:1) (183 mg, 63%). M.p. 258 °C. IR: ν_{max} (KBr)/cm^{-1}: 2961, 1614, 1403, 1324, 1256, 1167, 1123, 1067, 1020, 852, 623 and 436. ^{1}H NMR (400 MHz, $CDCl_3$): δ = 1.38 (s, 9H, *t*Bu), 7.73–7.84 (m, 16 H, Ar-*H*), 7.94 (s, 1 H, pyrene-*H*), 8.05 (s, 2 H, pyrene-H) and 8.25 (s, 2 H, pyrene-*H*) ppm; ^{13}C NMR (100 MHz, $CDCl_3$): δ = 149.7, 144.4, 144.1, 139.3, 136.2, 130.9, 130.8, 130.3, 130.0, 129.3, 127.4, 125.6, 125.54, 125.51, 125.4, 125.3, 125.2, 125.16, 124.7, 123.9, 122.8, 121.8, 35.5 and 31.6 ppm. FABMS: *m/z*: 834.29 [M^+]. $C_{48}H_{30}F_{12}$ (834.73): calcd C 69.07, H 3.62; found: C 68.97, H 3.83.

7-*tert*-Butyl-tetrakis-1,3,5,9-(4-cyanophenyl)pyrene (4e). Colourless prisms (CH_2Cl_2–methanol, 2:1) (144 mg, 62%). M.p. 378 °C. IR: ν_{max} (KBr)/cm^{-1}: 2954, 2230, 1683, 1604, 1504, 1480, 1256, 1178, 1109, 995, 898, 837 and 562. ^{1}H NMR (400 MHz, $CDCl_3$): δ = 1.37 (s, 9H, *t*Bu), 7.73 (d, *J* = 8.2 Hz, 4 H, Ar-*H*), 7.78 (d, *J* = 8.2 Hz, 4 H, Ar-*H*), 7.87 (d, *J* = 8.2 Hz, 4 H, Ar-*H*), 7.88 (d, J = 8.1 Hz, 4 H, Ar-*H*), 7.92 (s, 1 H, pyrene-*H*), 7.98 (s, 2 H, pyrene-*H*) and 8.21 (s, 2 H, pyrene-*H*) ppm. ^{13}C NMR (100 MHz, $CDCl_3$): δ = 147.5, 142.7, 142.4, 136.8, 133.4, 129.9, 128.5, 128.1, 127.1, 126.4, 124.8, 122.4, 122.2, 121.2, 119.4, 116.0, 115.96, 109.4, 109.2, 33.0 and 29.0 ppm. FABMS: *m/z*: 662.31 [M^+]. $C_{48}H_{30}N_4$ (662.78): calcd C 86.98, H 4.56; found: C 86.68, H 4.88.

7-*tert*-Butyl-1,3,5,9-tetrakis(4-formylphenyl)pyrene (4f). Yellow prisms (CH_2Cl_2–methanol, 2:1) (168 mg, 72%). M.p. 302 °C. IR: ν_{max} (KBr)/cm^{-1}: 3444, 2957, 1703, 1607, 1564, 1385, 1313, 1209, 1167, 819 and 490. H NMR (400 MHz, $CDCl_3$): δ = 1.37 (s, 9 H, *t*Bu), 7.81 (d, *J* = 8.1 Hz, 4H, Ar-*H*), 7.87 (d, *J* = 8.1 Hz, 4H, Ar-*H*), 8.00 (s, 1H, pyrene-*H*), 8.07–8.09 (m, 8H, Ar-*H*, 2H, pyrene-H), 8.28 (s, 2H, pyrene-*H*), 10.14 (s, 2H, C*H*O) and 10.16 (s, 2H, C*H*O) ppm. ^{13}C NMR (100 MHz, $CDCl_3$): δ = 191.82, 191.77, 149.8, 147.1, 146.8, 139.6, 136.5, 135.7, 135.5, 131.2, 130.7, 130.0, 129.9, 129.0, 128.9, 127.5, 125.3, 124.8, 123.9, 122.0, 35.5 and 31.6 ppm. FABMS: *m/z*: 674.28 [M^+]. $C_{48}H_{34}O_4$ (674.78): calcd C 85.44, H 5.08; found: C 85.34, H 5.35.

Synthesis of 7-*tert*-butyl-1,3,5,9-tetrakis(4-hydroxyimino-phenyl)pyrene (5). A mixture of 7-*tert*-butyl-1,3,5,9-tetrakis(4-formylphenyl)pyrene **4f** (30 mg, 0.045 mmoL), hydroxylamine hydrochloride (60 mg, 0.86 mmol), sodium hydroxyde (30 mg, 0.75 mmoL) and 10 mL ethanol were refluxed for 12 h, and then cooled to room temperature. The solvent was removed *in vacuo* to leave the residue, which was washed with water and recrystallized from acetone to give **5** (23 mg, 70%) as a yellow solid. M.p. 214 °C. IR: ν_{max} (KBr)/cm^{-1}: 33465, 2974, 1756, 1630, 1371, 1249, 1218, 1072, 1009, 974, 943, 836, 730, 607, 568, 524 and 466. ^{1}H NMR (400 MHz, $CDCl_3$): δ = 1.29 (s, 9H, *t*Bu), 2.22 (s, 4H, *OH*), 7.34 (d, *J* = 8.0 Hz, 4H, Ar-*H*), 7.45 (d, *J* = 8.0 Hz, 4H, Ar-*H*), 7.53 (d, *J* = 8.0 Hz, 4H, Ar-*H*), 7.62, (s, 2H, pyrene-*H*), 7.66 (d, *J* = 8.0 Hz, 4H, Ar-*H*), 7.67 (s, 2H, -CH=N-*H*), 8.05 (s, 2H, -CH=N-*H*), 8.14 (d, *J* = 9.2 Hz, 2 H, pyrene-*H*)) and 8.24 (s, 2H, pyrene-*H*) ppm; ^{13}C NMR (100 MHz, $CDCl_3$): δ = 115.02, 150.0, 149.8, 143.3, 142.9, 140.7, 138.1, 133.9, 133.6, 131.9, 131.8, 131.5, 131.3, 130.0, 129.8, 128.3, 128.0, 127.9, 126.4, 125.7, 125.4, 122.7, 36.4 and 32.1 ppm. FABMS: *m/z*: 734.52 [M^+]. calcd $C_{48}H_{38}N_4O_4$ (734.84): C 78.45, H 5.21; found: C 78.20, H 5.25.

Synthesis of 1,3,5,9-tetrakisphenylpyrene (6). A mixture of 7-*tert*-butyl-1,3,5,9-tetrakisphenylpyrene **4a** (50 mg, 0.09 {more s.f needed} mmoL), Nafion-H (50 mg), and 2 mL *o*-xylene were refluxed for 24 h, and then cooled to room temperature. The solid was removed *in vacuo* and the mother solution collected. The crude product was purified by column chromatography using dichloromethane–hexane (1:1) as eluent to afford a yellow solid. Recrystallization from a mixture of CH_2Cl_2–ethanol (2:1) gave **6** (23 mg, 51%) as light yellow prisms. M.p. 244 °C. IR: ν_{max} (KBr)/cm^{-1}: 3058, 3032, 1600, 1486, 1442, 1071, 1034, 893, 790, 759, 740, 700, 620 and 475. ^{1}H NMR (400 MHz, $CDCl_3$): δ = 7.42-7.45 (m, 4H, Ar-*H*), 7.49–7.53 (m, 8H, Ar-*H*), 7.59–7.61 (m, 4H, Ar-*H*), 7.66-7.68 (m, 4H, Ar-*H*), 7.85-7.89, (m, 1H, pyrene-*H*), 8.00 (s, 1H, pyrene-*H*), 8.17 (s, 2H, pyrene-*H*) and 8.14 (d, *J* = 8 Hz, 2H, pyrene-*H*)) ppm; ^{13}C NMR (100 MHz, $CDCl_3$): δ =141.2, 141.0, 139.6, 137.4, 130.7, 130.6, 130.1, 130.0, 128.4, 128.3, 127.4, 127.39, 127.2, 125.7, 125.5 and 124.1 ppm. FABMS: *m/z*: 506.12 (M^+). $C_{40}H_{26}$ (506.20): calcd C 94.83, H 5.17; found: C 94.77, H 5.29.

Acknowledgements

This work was performed under the Cooperative Research Program of "Network Joint Research Center for Materials and Devices (Institute for Materials Chemistry and Engineering, Kyushu University)". We would like to thank the OTEC at Saga University and the International Collaborative Project Fund of Guizhou province at Guizhou University for financial support. We also would like to thank the EPSRC and The Royal Society for financial support (travel grants to C.R.).

Notes

[a] *Department of Applied Chemistry, Faculty of Science and Engineering, Saga University, Honjo-machi 1, Saga 840-8502 Japan, E-mail: yamatot@cc.saga-u.ac.jp*

[b] *Emergent Molecular Function Research Group, RIKEN Center for Emergent Matter Science (CEMS), Wako, Saitama 351-0198, Japan, E-mail: jian-yong.hu@riken.jp*

[c] *Department of Chemistry, The University of Hull, Cottingham Road, Hull, Yorkshire, HU6 7RX, UK.*

[d] *Chemistry Department, Loughborough University, Loughborough, LE11 3TU, UK.*

†Electronic Supplementary Information (ESI) available: ^{1}H/^{13}C NMR spectra of **4a-f**, **5** and **6**, the effect of different solvents on the fluorescence emission spectra of **4** and **5**, etc. See DOI: 10.1039/b000000x/

References

1 (a) P. Tyagi, A. Venkateswararao and K. R. J. Thomas, *J. Org. Chem.*, 2011, **76**, 4571–4581; (b) L. Schmidt-Mende, A. Fechtenkötter, K.

Müllen, E. Moons, R. H. Friend and J. D. MacKenzie, *Science*, 2001, **293**, 1119–1122.
2 (a) X.-L. Feng, W. Pisula and K. Müllen, *Pure Appl. Chem.*, 2009, **81**, 2203–2224; (b) H. Klauk, D. J. Gundlach, J. A. Nichols and T. N. Jackson, *IEEE T ELECTRON DEV.*, 1999, **46**, 1258–1263; (c) S.-L. Suraru, U. Zschieschang, H. Klauk and F. Würthner, *Chem. Commum.*, 2011, **47**, 11504–11506.
3 (a) M. A. Baldo, D. F. O'Brien, Y. You, A. Shoustikov, S. Sibley, M. E. Thompson and S. R. Forrest, *Nature*, 1998, **395**, 151–154; (b) C.-T. Chen, *Chem. Mater*., 2004, **16**, 4389–4400.
4 (a) T. M. Figueira-Duarte and K. Müllen, *Chem. Rev*., 2011, **111**, 7260–7314; (b) J.-Y. Hu and T. Yamato, *Organic Light Emitting Diode - Material, Process and Devices*. **2011**, 21–60; (c) J.-Y. Hu, Y.-J. Pu, G. Nakata, S. Kawata, H. Sasabe and J. Kido, *Chem. Commun*., 2012, **48**, 8434–8436.
5 (a) Y.-L. Fogel, M. Kastler, Z.-H. Wang, D. Andrienko, G. J. Bodwell and K. Müllen, *J. Am. Chem. Soc*., 2007, **129**, 11743–11749; (b) K. Mochida, K. Kawasumi, Y. Segawa and K. Itami, *J. Am. Chem. Soc.*, 2011, **133**, 10716–10719; (c) B.-X. Gao, M. Wang, Y.-X. Cheng, L.-X. Wang, X.-B. Jing and F.-S. Wang, *J. Am. Chem. Soc.*, 2008, **130**, 8297–8306.
6 (a) X.-L. Ni, S. Wang, X. Zeng, Z. Tao and T. Yamato, *Org. Lett*., 2011, **13**, 552–555; (b) X.-L Ni, X. Zeng, C. Redshaw and T. Yamato, *J. Org. Chem.*, 2011, **76**, 5696–5702; (c) X.-L Ni, X. Zeng, C. Redshaw and T. Yamato, *Tetrahedron*, 2011, **67**, 3248–3253.
7 I. B. Berlman, *J. Phys. Chem.*, 1970, **74**, 3085–3093.
8 P. Sonar, M. S. Soh, Y. H. Cheng, J. T. Henssler and A. Sellinger, *Org. Lett.*, 2010, **15**, 3292–3295.
9 W. Sotoyama, H. Sato, M. Kinoshita, T. Takahashi, A. Matsuura, J. Kodama, N. Sawatari and H. Inoue, *SID Symposium Digest of Technical Papers*, 2003, **34**, 1294–1297.
10 (a) J.-Y. Hu, M. Era, M. R. J. Elsegood and T. Yamato, *Eur. J. Org. Chem.*, 2010, 72–79; (b) J.-Y. Hu, X.-L. Ni, X. Feng, M. Era, M. R. J. Elsegood, S. J. Teat and T. Yamato, *Org. Biomol. Chem*., 2012, **10**, 2255–2262; (c) X. Feng, J.-Y. Hu, L. Yi, N. Seto, Z. Tao, C. Redshaw, M. R. J. Elsegood and T. Yamato, *Chem.–Asian J*., 2012, **7**, 2854–2863.
11 X. Feng, J.-Y. Hu, F. Iwanaga, N. Seto, C. Redshaw, M. R. J. Elsegood and T. Yamato, *Org. Lett*., 2013, **15**, 1318–1321.
12 M. Tasashi and T. Yamato, *J. Org. Chem.*, 1983, **48**, 1461–1468.
13 (a) T. Yamato, C. Hideshima, A. Miyazawa, M. Tashiro, G. K. S. Prakash and G. A. Olah, *Catal. Lett.*, 1990, **6**, 345-348; (b) G. A. Olah, G. K. S. Prakash, P. S. Iyer, M. Tashiro, and T. Yamato, *J. Org. Chem.*, 1987, **52**, 1881–1884; (c) T. Yamato, C. Hideshima, M. Tashiro, G. K. S. Prakash and G.A. Olah, *J. Org. Chem.*, 1991, **56**, 6248–6250; (d) T. Yamato, *J. Synth. Org. Chem. Jpn.*, 1995, **53**, 487–499; (e) T. Yamato and J. Hu, *J. Chem. Res.*, 2006, 762–765.
14 C.-J. Chen, H.-J. Yen, W.-C. Chen and G.-S. Liou, *J. Polym. Sci., Part A: Polym. Chem.*, 2011, **49**, 3709–3718.
15 A. G. Crawford, A. D. Dwyer, Z.-Q. Liu, A. Steffen, A. Beeby, L.-O. Pålsson, D. L. Tozer and T. B. Marder, *J. Am. Chem. Soc*., 2011, **133**, 13349–13362.
16 J. N. Moorthy, P. Natarajan, P. Venkatakrishnan, D.-F. Huang and T. J. Chow, *Org. Lett.*, 2007, **9**, 5215–5218.
17 E. M. S. Castanheira, M. S. D. Carvalho, D. J. G. Soares, P. J. G. Coutinho, R. C. Calhelha and M-J. R. P. Queiroz, *J. Fluorescence*, 2011, **21**, 911–922.
18 (a) F. Han, L. Chi, W. Wu, X. Liang, M. Fu, J .Zhao, *J. Photochem. Photobio. A: Chem.*, 2008, **196**, 10-23. (b) G.-J. Zhao, J.-Y. Liu, L.-C. Zhou, K.-L. Han, *J. Phys. Chem. B*, 2007, **111**, 8940-8945.
19 J. C. Sciano, *Handbook of Organic Photochemistry*; CRC Press: Boca Raton, FL, 1989.
20 M. J. Frisch, G. W. Trucks, H. B. Schlegel, G. E. Scuseria, M. A. Robb, J. R. Cheeseman, J. A., Jr. Montgomery, T. Vreven, K. N. Kudin, J. C. Burant, J. M. Millam, S. S. Iyengar, J. Tomasi, V. Barone, B. Mennucci, M. Cossi, G. Scalmani, N. Rega, G. A. Petersson, H. Nakatsuji, M. Hada, M. Ehara, K. Toyota, R. Fukuda, J. Hasegawa, M. Ishida, T. Nakajima, Y. Honda, O. Kitao, H. Nakai, M. Klene, X. Li, J. E. Knox, H. P. Hratchian, J. B. Cross, V. Bakken, C. Adamo, J. Jaramillo, R. Gomperts, R. E. Stratmann, O. Yazyev, A. J. Austin, R. Cammi, C. Pomelli, J. W. Ochterski, P. Y. Ayala, K. Morokuma, G. A. Voth, P. Salvador, J. J. Dannenberg, V. G. Zakrzewski, S. Dapprich, A. D. Daniels, M. C. Strain, O. Farkas, D. K. Malick, A. D. Rabuck, K. Raghavachari, J. B. Foresman, J. V. Ortiz, Cui, Q.; Baboul, A. G.; Clifford, S.; Cioslowski, J.; Stefanov, B. B.; G. Liu, A. Liashenko, P. Piskorz, I. Komaromi, R. L. Martin, D. J. Fox, T. Keith, M. A. Al-Laham, C. Y. Peng, A. Nanayakkara, M. Challacombe, P. M. W. Gill, B. Johnson, W. Chen, M. W. Wong, C. Gonzalez and J. A. Pople, *Gaussian 03*, revision C.02, Gaussian, Inc., Wallingford CT, **2004**.
21 Y. Miura, E. Yamano, A. Tanaka and J. Yamauchi, *J. Org. Chem*., 1994, **59**, 3294–3300.